



# Non-linear analysis of plates by the analog equation method

J.T. Katsikadelis, M.S. Nerantzaki

*Department of Civil Engineering, National  
Technical University, Zografou Campus,  
GR-15773 Athens, Greece*

## ABSTRACT

The Analog Equation Method is applied to large deflection analysis of thin elastic plates. The von-Kármán plate theory is adopted. The deflection and the stress function of the non-linear problem are established by solving two linear uncoupled plate bending problems under the same boundary conditions subjected to "appropriate" (equivalent) fictitious loads. Numerical examples are presented which illustrate the efficiency and the accuracy of the proposed method.

## INTRODUCTION

Many methods have been developed to study large deflections of plates. Analytic as well approximate methods have been presented over the years [1]. However, all these methods are restricted to plates of specific simple geometry and boundary conditions. Realistic engineering problems are solved only by numerical methods such as FDM, FEM and BEM. The latter has been proven an efficient alternative to the domain type methods and has been used to study large deflection of plates in the last decade [2-8]. In this paper a novel solution approach to large deflection analysis of plates is presented. In what it follows the proposed method will be referred to as Analog Equation Method [9]. According to this method the non-linear problem governed by the coupled von-Kármán equations is substituted by two linear uncoupled plate bending problems subjected to "appropriate" equivalent fictitious load distributions under the same boundary conditions. Subsequently, using BEM for the non-homogeneous biharmonic equation, the deflection and the stress function as well as their second derivatives are expressed in terms of the unknown domain fictitious loads. Substituting the foregoing quantities into the von-Kármán equations yields a set of non-linear algebraic equations which permit the determination of the fictitious equivalent loads. The resulting non-linear equations are solved numerically by step increasing the actual load. The method is utilized to analyze certain example problems. The obtained numerical results are in excellent agreement when compared



with those obtained from other computational techniques. The proposed method can be categorized into BEM type methods as its implementation is based on BEM.

## GOVERNING EQUATIONS

The non-linear bending of thin plates is described by the von-Kármán equations [1]. Thus,

$$\nabla^4 w = \frac{g}{D} + \frac{h}{D} L(w, F) \quad (1)$$

$$\nabla^4 F = -\frac{E}{2} L(w, w) \quad \text{in } \Omega \quad (2)$$

in which  $\Omega$  is a two dimensional region with boundary  $\Gamma$  occupied by the plate;  $w = w(x, y)$ ,  $(x, y) \in \Omega$ , is the transverse deflection;  $F = F(x, y)$  is the Airy's stress function;  $D = Eh^3 / 12(1 - \nu^2)$  the flexural rigidity of the plate, having thickness  $h$  and elastic constants  $E, \nu$ ;  $\nabla^4$  is the biharmonic operator and  $L(, )$  is a non-linear operator applied to the functions  $w$  and  $F$  and represents

$$L(w, F) = w_{,xx} F_{,yy} + w_{,yy} F_{,xx} - 2w_{,xy} F_{,xy} \quad (3)$$

$L(w, w)$  is obtained by replacing  $F$  with  $w$  in equation (3), i.e.

$$L(w, w) = 2(w_{,xx} w_{,yy} - w^2_{,xy}) \quad (4)$$

The functions  $L(w, F)$  and  $L(w, w)$  define the non-linearity of the problem which is due to the coupling of the transverse deflection with the membrane deformation.

The stress resultants at a point  $x, y \in \Omega$  are given in terms of  $w$  and  $F$  as

$$\begin{aligned} M_x &= -D(w_{,xx} + \nu w_{,yy}) \\ M_y &= -D(w_{,yy} + \nu w_{,xx}) \\ M_{xy} &= D(1 - \nu)w_{,xy} \\ Q_x &= -D(\nabla^2 w)_{,x} \\ Q_y &= -D(\nabla^2 w)_{,y} \\ N_x &= hF_{,yy} \\ N_y &= hF_{,xx} \\ N_{xy} &= -hF_{,xy} \end{aligned} \quad (5)$$



In equations (5)  $M_x, M_y$  are the bending moments,  $M_{xy}$  is the twisting moment,  $Q_x, Q_y$  are the transverse shearing forces and  $N_x, N_y, N_{xy}$  are the membrane forces.

The plate is subjected to the following boundary conditions on the boundary  $\Gamma$

$$\alpha_1 w + \alpha_2 V^* w = \alpha_3 \quad (6a)$$

$$\beta_1 w_{,n} + \beta_2 M w = \beta_3 \quad (6b)$$

$$F = \gamma_1 \quad (7a)$$

$$F_{,n} = \gamma_2 \quad (7b)$$

where  $\alpha_i = \alpha_i(s)$ ,  $\beta_i = \beta_i(s)$ , ( $i = 1, 2, 3$ ) and  $\gamma_k = \gamma_k(s)$  ( $k = 1, 2$ ) are functions specified on  $\Gamma$ .  $V^* w$  and  $M w$  are the reactive equivalent transverse force and the bending moment along the boundary given as [6]

$$V^* w = V w + N_n w_{,n} + N_{nt} w_{,t} \quad (8a)$$

$$M w = -D(w_{,nn} + \nu w_{,tt}) \quad (8b)$$

where

$$V w = -D[(\nabla^2 w)_{,n} - (\nu - 1)(w_{,nt})_{,t}] \quad (9)$$

is the equivalent reactive force of the linear theory. The remaining terms in equation (8a) are due to the contribution of the membrane force components  $N_n, N_{nt}$  in the transverse direction.

Using intrinsic co-ordinates, that is the distance along the normal  $n$  to the boundary and the arc length  $s$ , and taking into account that

$$\frac{\partial}{\partial t} = \frac{\partial}{\partial s} \quad (10a)$$

$$\frac{\partial^2}{\partial t^2} = \frac{\partial^2}{\partial s^2} + \kappa \frac{\partial}{\partial n} \quad (10b)$$

$$\frac{\partial^2}{\partial n \partial t} = \frac{\partial^2}{\partial s \partial n} - \kappa \frac{\partial}{\partial s} \quad (10c)$$



in which  $\kappa(s)$  is the curvature of the boundary, equations (8a,b) are written as

$$V^*w = -D[\Psi - (\nu - 1)(X_{,s} - \kappa\Omega_{,s}), ] + N_n X + N_{nt}\Omega_{,s} \quad (11a)$$

$$Mw = -D[\Phi + (\nu - 1)(\Omega_{,ss} + \kappa X)] \quad (11b)$$

where the following notation has been used

$$\Omega = w \quad X = w_{,n} \quad \Phi = \nabla^2 w \quad \Psi = (\nabla^2 w)_{,n} \quad (12)$$

It is apparent from equations (6a,b) that all types of boundary conditions with respect to the transverse deflection  $w$  can be treated by specifying appropriately the functions  $\alpha_i, \beta_i$ . On the other hand stress boundary conditions are considered for the membrane stresses which are rather more easily expressible in terms of the stress function (as it is the case of movable edges or edges subjected to prescribed inplane edge forces).

#### THE ANALOG EQUATION METHOD

The boundary value problem described by equations (1),(2),(6a,b) and (7a,b) is solved using the Analog Equation Method (AEM) developed by Katsikadelis [9]. In the problem at hand this method is applied as following:

Let  $w$  and  $F$  be the sought solution to equations (1) and (2). These functions are four times continuously differentiable with respect to the co-ordinates  $x,y$  in  $\Omega$  and three times on its boundary  $\Gamma$ . If the biharmonic operator is applied to these functions we have

$$\nabla^4 w = q(x,y) \quad (13a)$$

$$\nabla^4 F = \bar{q}(x,y) \quad (13b)$$

Equations (13a,b) indicate that the solution to the original problem (1), (2) can be obtained as the solution of two uncoupled linear plate bending problems with unit stiffness and subjected to the equivalent fictitious loads  $q$  and  $\bar{q}$  under the given boundary conditions.

According to the AEM the unknown load distributions  $q$  and  $\bar{q}$  can be established using BEM which is applied as following:

For any function  $w$  satisfying the non-homogeneous biharmonic equation (13a) the following integral representations are obtained [10].



$$\varepsilon w(P) = \int_{\Omega} \Lambda_4 q d\Omega - \int_{\Gamma} (\Lambda_1 \Omega + \Lambda_2 X + \Lambda_3 \Phi + \Lambda_4 \Psi) ds \quad (14)$$

$$\varepsilon \nabla^2 w(P) = \int_{\Omega} \Lambda_2 q d\Omega - \int_{\Gamma} (\Lambda_1 \Phi + \Lambda_2 \Psi) ds \quad (15)$$

where  $\varepsilon = 1, 1/2, 0$  depending on whether the point  $P$  is inside the domain  $\Omega$ , on the boundary  $\Gamma$  or outside  $\Omega$ , respectively. Note that the boundary has been assumed to be smooth at the point  $P$ . The kernels  $\Lambda_i = \Lambda_i(r)$ ,  $r = |P - q|$ ,  $P \in \Omega$ ,  $q \in \Gamma$ , are given as

$$\Lambda_1(r) = -\frac{\cos \varphi}{r} \quad (16a)$$

$$\Lambda_2(r) = \ell nr + 1 \quad (16b)$$

$$\Lambda_3(r) = -\frac{1}{4}(2r\ell nr + r)\cos\varphi \quad (16c)$$

$$\Lambda_4(r) = \frac{1}{4}r^2\ell nr \quad (16d)$$

$$\varphi = r, \hat{n}.$$

The boundary conditions (6a,b) and the integral representations (14) and (15) for  $P \in \Gamma$  constitute a set of four boundary equations with respect to the boundary quantities  $\Omega$ ,  $X$ ,  $\Phi$ ,  $\Psi$ . Two of these equations are boundary integral equations and the remaining boundary differential. These equations are solved numerically. Thus, approximating the boundary integrals using the boundary element technique, the domain integrals using domain nodal points (e.g. FEM discretization or Gauss integration) and the boundary derivatives using finite differences, the following set of linear equations is obtained:

$$\begin{bmatrix} [A_{11}] & [A_{12}] & [0] & [A_{14}] \\ [A_{21}] & [A_{22}] & [A_{23}] & [0] \\ [A_{31}] & [A_{32}] & [A_{33}] & [A_{34}] \\ [0] & [0] & [A_{43}] & [A_{44}] \end{bmatrix} \begin{Bmatrix} \{\Omega\} \\ \{X\} \\ \{\Phi\} \\ \{\Psi\} \end{Bmatrix} = \begin{Bmatrix} \{B_1\} \\ \{B_2\} \\ \{0\} \\ \{0\} \end{Bmatrix} + \begin{bmatrix} 0 \\ 0 \\ [C_3] \\ [C_4] \end{bmatrix} \{q\} \quad (17)$$

where  $[A_{ij}]$  ( $i, j=1,2,3,4$ ) are  $N \times N$  known coefficient matrices,  $\{B_i\}$  ( $i=1,2$ )  $N \times 1$  known constant column matrices and  $[C_i]$  ( $i=3,4$ )  $N \times M$  known coefficient matrices.  $\{\Omega\}, \{X\}, \{\Phi\}, \{\Psi\}$  are  $N \times 1$  vectors including the nodal values of the unknown boundary quantities, while  $\{q\}$  is an  $M \times 1$  vector including the nodal values



of the unknown fictitious loading.  $N$  is the number of the boundary nodal points, whereas  $M$  is the number of the domain nodal points.

Equation (17) permits the elimination of the boundary quantities  $\Omega, X, \Phi, \Psi$  from the discretized counterpart of equation (14), which after collocation at the  $M$  domain nodal Gauss points yields

$$\{w\} = [G]\{q\} \quad (18)$$

where  $\{w\}$  is an  $M \times 1$  vector including the values of the function  $w$  at the  $M$  Gauss integrations points and  $[G]$  is an  $M \times M$  known coefficient matrix.

Subsequent differentiation of equation (14) twice with respect to  $x$  and  $y$  yields

$$\begin{aligned} w_{,xx}(P) &= \int_{\Omega} (\Lambda_4)_{,xx} q d\Omega \\ &\quad - \int_{\Gamma} [(\Lambda_1)_{,xx} \Omega + (\Lambda_2)_{,xx} X + (\Lambda_3)_{,xx} \Phi + (\Lambda_4)_{,xx} \Psi] ds \end{aligned} \quad (19a)$$

$$\begin{aligned} w_{,yy}(P) &= \int_{\Omega} (\Lambda_4)_{,yy} q d\Omega \\ &\quad - \int_{\Gamma} [(\Lambda_1)_{,yy} \Omega + (\Lambda_2)_{,yy} X + (\Lambda_3)_{,yy} \Phi + (\Lambda_4)_{,yy} \Psi] ds \end{aligned} \quad (19b)$$

$$\begin{aligned} w_{,xy}(P) &= \int_{\Omega} (\Lambda_4)_{,xy} q d\Omega \\ &\quad - \int_{\Gamma} [(\Lambda_1)_{,xy} \Omega + (\Lambda_2)_{,xy} X + (\Lambda_3)_{,xy} \Phi + (\Lambda_4)_{,xy} \Psi] ds \end{aligned} \quad (19c)$$

The derivatives of the kernels are given in the Appendix.

Elimination of the boundary quantities from the discretized counterparts of equations (19a,b,c) using equations (17) and collocation at the  $M$  Gauss integration points inside  $\Omega$  yield

$$\{w_{xx}\} = [G_{xx}]\{q\} \quad (20)$$

$$\{w_{yy}\} = [G_{yy}]\{q\} \quad (21)$$

$$\{w_{xy}\} = [G_{xy}]\{q\} \quad (22)$$

where  $[G_{xx}]$ ,  $[G_{yy}]$ ,  $[G_{xy}]$  are known  $M \times M$  coefficient matrices. Equations (18),(20)-(22) are valid for homogeneous boundary conditions. For non-homogeneous boundary conditions an additive constant vector will appear.

Analogous relations can be derived for the function  $F$ . They differ only in the boundary conditions. However, equations (7a,b) is a special case of (6a,b), that is they are obtained by specifying  $\alpha_1 = 1$ ,  $\alpha_2 = 0$ ,  $\alpha_3 = \gamma_1$ ,  $\beta_1 = 1$ ,  $\beta_2 = 0$ ,  $\beta_3 = \gamma_2$ . Consequently, only the upper half part of equation (17) is affected. Thus, we have

$$\{F\} = [\bar{G}]\{\bar{q}\} \quad (23)$$

$$\{F_{xx}\} = [\bar{G}_{xx}]\{\bar{q}\} \quad (24)$$

$$\{F_{yy}\} = [\bar{G}_{yy}]\{\bar{q}\} \quad (25)$$

$$\{F_{xy}\} = [\bar{G}_{xy}]\{\bar{q}\} \quad (26)$$

The matrices  $[\bar{G}]$ ,  $[\bar{G}_{xx}]$ ,  $[\bar{G}_{yy}]$ ,  $[\bar{G}_{xy}]$  are defined similar to  $[G]$ ,  $[G_{xx}]$ ,  $[G_{yy}]$  and  $[G_{xy}]$ .

The final step of AEM is to apply equations (1) and (2) to the  $M$  nodal integration points inside the domain  $\Omega$ . This yields

$$\{\nabla^4 w\} = \frac{1}{D}\{g\} + \frac{h}{D}\{L(w, \dot{F})\}$$

$$\{\nabla^4 F\} = -\frac{E}{2}\{L(w, w)\}$$

which by means of equations (13a,b), (18) and (20)-(26) become

$$D\{q\} - h\{L(q, \bar{q})\} = \{g\} \quad (27)$$

$$\{\bar{q}\} = -\frac{E}{2}\{L(q, q)\} \quad (28)$$

Equations (27) and (28) are solved numerically by step increasing the load.

## NUMERICAL RESULTS

On the basis of analysis presented in previous sections a computer program has been written and some example plates have been studied to illustrate the efficiency of the developed method and investigate its accuracy.

**Example 1**

A circular uniformly-loaded plate with clamped stress-free edge (i.e.,  $w = 0$ ,  $w_{,n} = 0$ ,  $F = 0$ ,  $F_{,n} = 0$ ) has been studied. The data of the plate are  $a/h = 50$ ,  $\nu = 0.30$ ,  $g = \text{constant}$ . The obtained numerical results are presented in Table 1. They are compared with those obtained from a BEM solution as well as with those from an analytical solution and are found in excellent agreement. In Figures 1 and 2 the distributions of the fictitious loads  $q = q(r)$  and  $\bar{q} = \bar{q}(r)$  along the diameter of the plate are shown. From Figure 1 it can be concluded that for small values of the actual load, the fictitious load  $q$  is constant and equal to  $g$  (linear behaviour). However, as  $g$  increases  $q$  is no more constant. It exhibits peaks which are shifted away from the center. The distribution takes place so that

$$2\pi \int_0^a q(r) dr = \pi a^2 g$$

The same is valid for the fictitious load  $\bar{q}$ . The total load in this case is equal to zero

$$2\pi \int_0^a \bar{q}(r) dr = 0$$

This was anticipated since  $L(w, w)$  is the second invariant of the curvature tensor of the deflection surface  $w$  and it can be proven that in this case it satisfies the relation

$$\int_{\Omega} L(w, w) d\Omega = 0$$

**Example 2**

A circular plate with simply-supported stress-free edge ( $w = 0, M_n = 0$ ,  $F = 0, F_{,n} = 0$ ) has been studied. The same data as in Example 1 have been used. Numerical results have been obtained for two values of the load  $g$ . They are presented in Table 2 as compared with those obtained from a BEM solution.

**Example 3**

A square uniformly loaded plate with clamped stress-free edges has been analyzed. The obtained numerical results are presented in Figure 3 and in Table 3. The data of the plate are  $a/h = 100$ ,  $\nu = 0.30$ . They are in full agreement with those obtained using BEM [6].

**Example 4**

A square uniformly loaded plate with simply supported stress-free edge has been analyzed. The same data as in Example 3 have been used. The obtained numerical results are given in Figure 4 and in Table 4. They are in full agreement with those obtained using BEM [6].



In Table 3 and 4 the values obtained by BEM [6] are not shown as they differ negligibly.

## CONCLUSIONS

A novel BEM solution, the Analog Equation Method, has been presented for non-linear analysis of thin elastic plates. According to this formulation the coupled non-linear governing equations are substituted by two linear plate bending equations subjected to appropriate fictitious equivalent loads, which are established using BEM. Its efficiency and accuracy are demonstrated by analyzing several examples.

*Table 1. Deflections, membrane and bending stresses along the radius of a uniformly loaded circular plate with clamped stress-free edge ( $\nu = 0.30$ ,  $\alpha / h = 50$ ,  $g^* = g\alpha^4 / Eh^4 = 10$ ).*

$r/a$	$\bar{w} = w/h$			$\bar{\sigma}_r^m = \sigma_r^m a^2 / Eh^2$			$\bar{\sigma}_r^b = \sigma_r^b a^2 / Eh^2$		
	Anal.	BEM	AEM	Anal.	BEM	AEM	Anal.	BEM	AEM
	Ref.[11]	Ref.[6]		Ref.[11]	Ref.[6]		Ref.[11]	Ref.[6]	
0	1.310	1.308	1.307	0.782	0.780	0.780	3.250	3.253	3.253
0.098	1.290	1.286	1.286	0.770	0.768	0.768	3.214	3.208	3.207
0.305	1.105	1.101	1.102	0.666	0.664	0.664	2.821	2.812	2.810
0.562	0.660	0.658	0.659	0.420	0.415	0.415	1.214	1.218	-1.208
0.802	0.190	0.188	0.189	0.159	0.171	0.172	-2.285	-2.278	-2.266
0.960	0.010	0.009	0.009	0.026	0.026	0.026	-5.750	-5.777	-5.802

*Table 2. Deflections, membrane and bending stresses along the radius of a uniformly loaded circular plate with simply-supported stress-free edge ( $\nu = 0.30$ ,  $a/h = 50$ )*

$g^*$	$r/a$	$\bar{w} = w/h$		$\bar{\sigma}_r^m = \sigma_r^m a^2 / Eh^2$		$\bar{\sigma}_r^b = \sigma_r^b a^2 / Eh^2$	
		BEM Ref.[11]	AEM	BEM Ref.[11]	AEM	BEM Ref.[11]	AEM
5	0	1.805	1.805	0.855	0.854	2.599	2.599
	0.098	1.788	1.788	0.847	0.846	2.610	2.610
	0.305	1.635	1.635	0.777	0.776	2.701	2.700
	0.562	1.217	1.217	0.582	0.582	2.700	2.696
	0.802	0.606	0.607	0.287	0.286	1.934	1.932
	0.960	0.124	0.124	0.070	0.069	0.492	0.477
25	0	3.662	3.660	2.977	2.969	3.811	3.819
	0.098	3.636	3.634	2.957	2.951	3.897	3.904
	0.305	3.403	3.401	2.802	2.793	4.636	4.642
	0.562	2.696	2.691	2.304	2.290	6.530	6.516
	0.802	1.455	1.457	1.222	1.213	7.318	7.241
	0.960	0.305	0.310	0.286	0.290	2.295	2.164

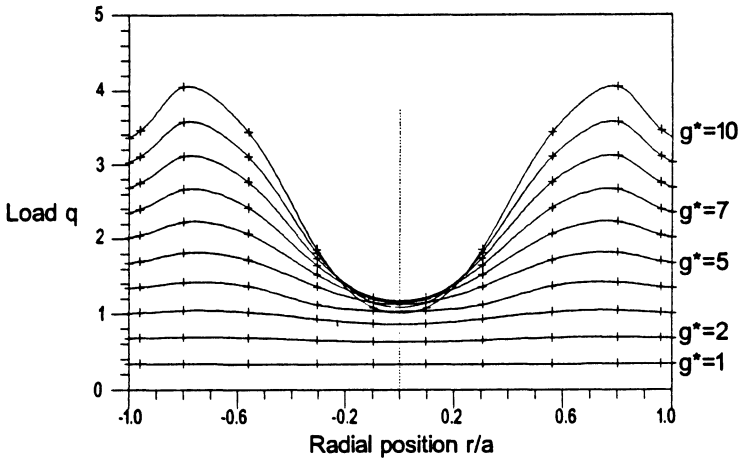


Fig.1 Distribution of the equivalent load  $q$  along the diameter of a clamped circular plate with movable edge for various values of the load ( $\nu = 0.30$ ,  $a/h = 50$ ,  $g^* = ga^4 / Eh^4 = 10$ ).

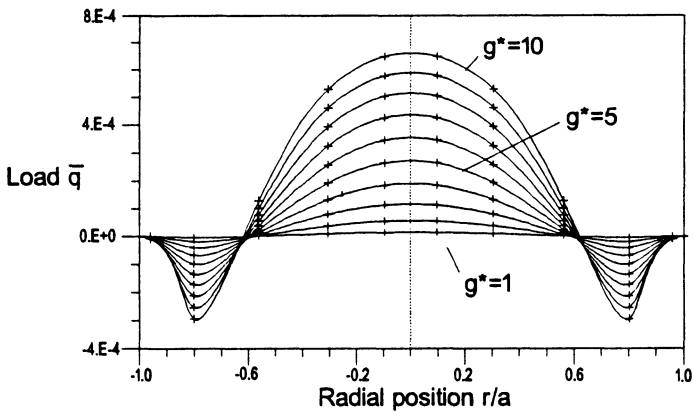


Fig.2 Distribution of the equivalent load  $\bar{q}$  along the diameter of a clamped circular plate with movable edge for various values of the load ( $\nu = 0.30$ ,  $a/h = 50$ ,  $g^* = ga^4 / Eh^4 = 10$ ).

*Table 3. Deflections, bending and membrane stresses along the half line  $x=0$  in a square uniformly loaded clamped square plate with stress-free edges ( $\nu = 0.30, a / h = 100$ )*

$g^*$	$y/a$	$\bar{w}$	$\bar{\sigma}_x^b$	$\bar{\sigma}_y^b$	$\bar{\sigma}_x^m$	$\bar{\sigma}_y^m$
128	0.049	1.355	11.574	11.697	2.695	2.762
	0.152	1.185	10.183	11.042	1.755	2.365
	0.281	0.745	5.687	5.831	-0.369	1.454
	0.401	0.232	-2.373	-9.762	-2.224	0.504
	0.480	0.013	-10.036	-29.661	-3.696	-0.258
192	0.049	1.779	13.976	14.210	4.363	4.451
	0.152	1.569	12.491	14.2301	2.984	3.824
	0.281	1.007	7.188	8.694	-0.427	2.370
	0.401	0.320	-3.452	-12.701	-3.736	0.824
	0.480	0.018	-13.793	-41.063	-6.490	-0.462

*Table 4. Deflections, bending and membrane stresses along the half line  $x=0$  in a square uniformly loaded simply supported square plate with stress-free edges ( $\nu = 0.30, a / h = 100$ )*

$g^*$	$y/a$	$\bar{w}$	$\bar{\sigma}_x^b$	$\bar{\sigma}_y^b$	$\bar{\sigma}_x^m$	$\bar{\sigma}_y^m$
128	0.049	2.652	11.842	12.140	5.214	5.195
	0.152	2.469	11.488	14.119	4.416	4.404
	0.281	1.913	9.997	16.924	1.112	2.524
	0.401	0.996	5.621	12.874	-5.467	0.721
	0.480	0.209	0.394	2.883	-11.662	0.061
192	0.049	3.262	13.099	13.515	7.243	7.162
	0.152	3.056	12.857	16.597	6.395	5.967
	0.281	2.403	11.645	21.891	1.943	3.224
	0.401	1.268	6.685	17.676	-7.933	0.868
	0.480	0.267	0.340	3.987	-17.071	0.087

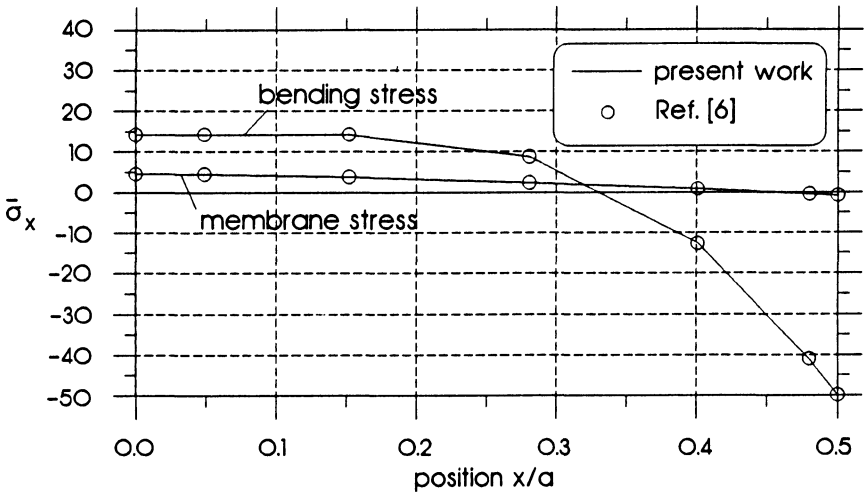


Fig.3. Variation of the membrane stresses  $\bar{\sigma}_x^m = \sigma_x^m a^4 / Eh^4$  and bending stress  $\bar{\sigma}_x^b = \sigma_x^b a^4 / Eh^4$  along the central half line  $y=0$ , in a clamped square plate with stress-free edges ( $\nu = 0.30$ ,  $a/h = 100$ ,  $g^* = ga^4 / Eh^4 = 192$ ).

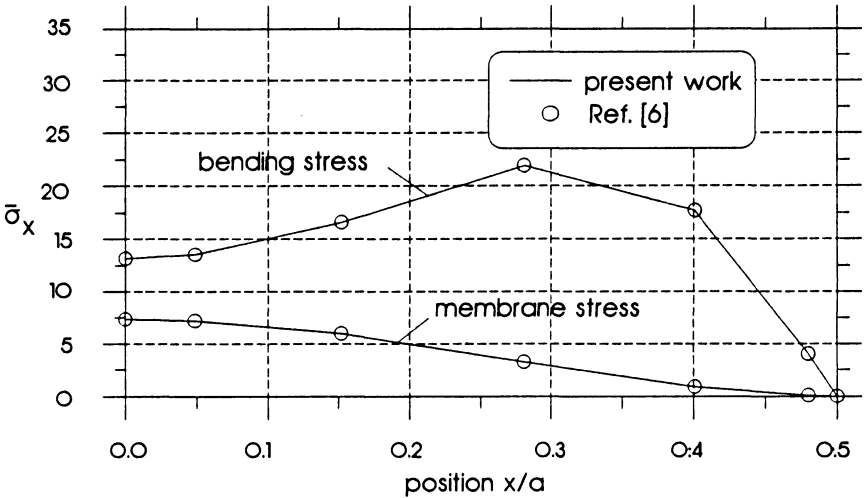


Fig.4. Variation of the membrane stresses  $\bar{\sigma}_x^m = \sigma_x^m a^4 / Eh^4$  and bending stress  $\bar{\sigma}_x^b = \sigma_x^b a^4 / Eh^4$  along the central half line  $y=0$ , in a simply supported square plate with stress-free edges ( $\nu = 0.30$ ,  $a/h = 100$ ,  $g^* = ga^4 / Eh^4 = 192$ ).



## REFERENCES

1. Chia, C.Y. 1980. Analysis of plates. New York: McGraw-Hill.
2. Tanaka, M. 1982. Integral equation approach to small and large displacements of thin elastic plates. *Boundary element methods in engineering*, p.526-539. Berlin. Springer-Verlag.
3. Kamiya, N. & Sawaki, Y. 1982. Integral formulation for non-linear bending of plates. *ZAMM* 62:651-655.
4. O'Donoghue, P.E. & Atluri, S.N. 1987. Field/ Boundary element approach to the large deflection of thin flat plates. *Comp. & Struc.* 27,3:427-435.
5. Nerantzaki, M.S. & Katsikadelis, J.T. 1988. A Green's function method for large deflection analysis of plates, *Acta Mech.* 25:211-225.
6. Katsikadelis, J.T. & Nerantzaki, M.S. 1988. Large deflections of thin plates by the boundary element method. In C.A Brebbia (ed.), *Boundary Elements X*, 3, p.435-456. Berlin, Springer-Verlag.
7. Kamiya N. 1988. Structural non-linear analysis by boundary element methods. In C.A. Brebbia (ed.), *Boundary elements X*, 3: p.17-27, Berlin, Springer-Verlag.
8. Elzein, A. & Syngellakis S. 1989. High-order elements for the BEM stability analysis of imperfect plates. In C.A. Brebbia & J.J. Connor (eds.), *Advances in boundary elements* 3, p.269-284. Berlin, Springer-Verlag.
9. Katsikadelis, J.T. 1993. The analog equation method, to be published.
10. Katsikadelis, J.T. & Armenakas, A.E. 1989. A new boundary equation solution to the plate problem. *ASME J. Appl. Mech.* 56:364-374.
11. Nerantzaki, M.S. 1992. Non-linear analysis of plates by the boundary element method, Ph.D. Dissertation, National Technical University, Athens.

## APPENDIX

a. Derivatives of the kernels  $\Lambda_i(r)$

$$\frac{\partial^2 \Lambda_1}{\partial x^2} = -\frac{2}{r^3} \cos(2\omega - \varphi) \quad (\text{A1a})$$

$$\frac{\partial^2 \Lambda_1}{\partial y^2} = \frac{2}{r^3} \cos(2\omega - \varphi) \quad (\text{A1b})$$

$$\frac{\partial^2 \Lambda_1}{\partial x \partial y} = -\frac{2}{r^3} \sin(2\omega - \varphi) \quad (\text{A1c})$$



$$\frac{\partial^2 \Lambda_2}{\partial x^2} = \frac{1}{r^2} (\sin^2 \omega - \cos^2 \omega) \quad (\text{A2a})$$

$$\frac{\partial^2 \Lambda_2}{\partial y^2} = \frac{1}{r^2} (\cos^2 \omega - \sin^2 \omega) \quad (\text{A2b})$$

$$\frac{\partial^2 \Lambda_2}{\partial x \partial y} = -\frac{\sin 2\omega}{r^2} \quad (\text{A2c})$$

$$\frac{\partial^2 \Lambda_3}{\partial x^2} = \frac{\sin \varphi \cos \omega \sin \omega}{r} - \frac{\cos \varphi}{2r} \quad (\text{A3a})$$

$$\frac{\partial^2 \Lambda_3}{\partial y^2} = -\frac{\sin \varphi \cos \omega \sin \omega}{r} - \frac{\cos \varphi}{2r} \quad (\text{A3b})$$

$$\frac{\partial^2 \Lambda_3}{\partial x \partial y} = -\frac{\sin \varphi \cos 2\omega}{2r} \quad (\text{A3c})$$

$$\frac{\partial^2 \Lambda_4}{\partial x^2} = \frac{1}{2} \ln r + \frac{1}{4} + \frac{1}{2} \cos^2 \omega \quad (\text{A4a})$$

$$\frac{\partial^2 \Lambda_4}{\partial y^2} = \frac{1}{2} \ln r + \frac{1}{4} + \frac{1}{2} \sin^2 \omega \quad (\text{A4b})$$

$$\frac{\partial^2 \Lambda_4}{\partial x \partial y} = \frac{1}{4} \sin 2\omega \quad (\text{A4c})$$

in which  $\omega = \hat{x}, r$  is the angle between the x-axis and the vector  $r$  and  $\varphi = \hat{r}, n$  is the angle between the vector  $r$  and the outward normal  $n$ .